We are IntechOpen,
the world's leading publisher of
Open Access books
Built by scientists, for scientists

6,900
Open access books available

185,000
International authors and editors

200M
Downloads

154
Countries delivered to

Our authors are among the

TOP 1%
most cited scientists

12.2%
Contributors from top 500 universities

Interested in publishing with us?
Contact book.department@intechopen.com

Numbers displayed above are based on latest data collected.
For more information visit www.intechopen.com

Multi-Sensor Feature Extraction and Data Fusion Using ANFIS and 2D Wavelet Transform in Structural Health Monitoring

Ponciano Jorge Escamilla-Ambrosio, Xuefeng Liu,
Juan Manuel Ramírez-Cortés,
Abraham Rodríguez-Mota and
María del Pilar Gómez-Gil

Additional information is available at the end of the chapter

Abstract

In this chapter, a novel feature extraction and data fusion approach for structural damage detection and localisation is presented. This approach combines adaptive network-based fuzzy inference systems (ANFIS) and two-dimensional wavelet transform (2D-WT) technologies. Simultaneous multi-sensor feature extraction and data fusion based on 2D-WT is carried out by forming a 2D multivariate signal, which is used to analyse the structure vibration response by measuring all sensors jointly. Energy values obtained from two-level db3 wavelet decomposition are arranged in a so-called energy percentage matrix (EPM), which is taken as an input for the ANFIS. The system is further trained by defining its output as the structural condition represented by a condition index. A set of output index patterns are defined depending on the level of damage assessment performed. The proposed method was tested through experiments using a cantilever beam structure. The testing results showed that the method is successful in detecting and localising damage by vibration analysis in structural health monitoring.

Keywords: sensor fusion, structural health monitoring, structural damage, ANFIS, 2D wavelet transform

1. Introduction

Structural health monitoring (SHM) refers to the process of damage detection, localization, quantification, or prediction, in infrastructure associated to fields such as aerospace, civil, or

mechanical engineering. In engineering structures, damage is regarded as changes to physical and/or geometric properties of these systems which adversely affect their current or future performance [1, 2]. The interest in the ability to detect and locate structural damage at the earliest possible stage relies on safety issues with a consequence in economic benefits. Damage identification methods can be classified into four levels of damage assessment: level 1 (detection): determination that damage is present in the structure; level 2 (localisation): level 1 plus determination of the geometric location of the damage; level 3 (quantification): level 2 plus quantification of the severity of the damage; and level 4 (prediction): level 3 plus prediction of the remaining service life of the structure [3–5]. A variety of signal processing techniques have been attempted with good results in the field of SHM, such as statistical time series models, Fourier analysis, Wigner-Ville transform, Cohen class, Hilbert-Huang transform and different variations of wavelet analysis [6]. Data interpretation includes approaches such as neural networks, support vector machine, fuzzy and neurofuzzy schemes, Bayesian classifiers, or hybrid classifiers [7–11]. Among these, wavelet techniques (WT) have been proven to be an effective approach for damage detection, based on their characteristics to analyse non-stationary signals in both time and frequency domains. This analytical tool has gained preference in the research community to explore its applicability to perform structural damage assessment. Therefore, a variety of wavelet-based methods for damage detection have been proposed [12–14]. These methods can be broadly classified into three categories [15]: (1) variation of wavelet coefficients, (2) local perturbation of wavelet coefficients in a space domain and (3) reflected wave caused by local damage. The first category is generally used to find the existence and severity of damage. The second category is used to localise the damage in structures. The third category is used to measure the severity as well as the location of damage.

Under the premise that damage (e.g., cracks) in a structure will cause structural response perturbations at damage sites, a number of wavelet-based variants have been reported in the last decade in the field of SHM. In Ref. [16], an algorithm based on the wavelet packet transform and the Karhunen-Loéve transform is used to decompose the signals coming from an accelerometer on a vibrating composite beam. Wavelet packet transform was used as a feature extraction tool in SHM with good results. Integration of the discrete wavelet transform, an autoregressive model, damage-sensitive features, and support vector machine are proposed in Ref. [17] as a novel and efficient framework for damage detection of smart structures. Winkelman et al. [18] reported a novel signal-processing technique based on wavelet thresholding/denoising and Gabor wavelet transform. A damage identification method using unsupervised blind source separation with a wavelet-based pre-processing is presented in Ref. [19]. The authors report that independent component analysis biases to extract sparse components from the observed mixture signals, revealing damage instant and location.

In this chapter, an approach to structural damage detection and localisation (i.e. level 1 and level 2 damage assessments) based on the combination of two-dimensional WT (2D-WT) and adaptive network-based fuzzy inference system (ANFIS) techniques is described. The main novelty of the proposed approach resides in using 2D-WT to simultaneously perform multi-sensor data fusion and feature extraction for structural damage detection and localisation purposes. In addition, the use of an ANFIS system provides a fuzzy index damage representation for simultaneous identification and location of the damage.

2. Background on 2D-WT and ANFIS

2.1. Wavelet transform (WT)

In the WT, a signal $f(t)$ is written as a series expansion in terms of wavelet families [20]:

$$f(t) = \sum_{k=-\infty}^{+\infty} <f(t), \varphi(t-k)> \varphi(t-k) + \\ \sum_{j=-\infty}^{-1} \sum_{k=-\infty}^{+\infty} <f(t), \psi_{j,k}(t)> \psi_{j,k}(t) \tag{1}$$

where the father wavelet family $\{\varphi(t-k), k \in Z\}$ is used to describe the smooth part of $f(t)$ and the mother wavelet family $\{\psi_{j,k}(t), j \geq 0\}$ is used to describe the details of $f(t)$ at different levels. This expansion can expose the information originally hidden in $f(t)$.

An efficient way to implement the WT, and its inverse (IWT), is to use filter banks and downsampling/upsampling techniques. Moreover, the connection of WT with filter banks is a tool to understand the frequency allocation property of WT. **Figure 1** shows a two-level discrete wavelet decomposition and reconstruction, which demonstrates the idea of using filter banks to calculate WT and IWT.

The original signal $f(t)$ is broken down into three sub-signals: A_2, D_1, and D_2. From $f(t)$ to A_2, D_2, and D_1, the whole process could be seen as passing $f(t)$ through three filters (see **Figure 1b**). Each filter has different frequency characteristics and thus a frequency allocation is achieved through wavelet analysis. For example, the spectrum of the three filters associated with a two-level Haar wavelet analysis is shown in **Figure 2**. Note that the spectrum is plotted over the range [0, 0.5], where 0.5 corresponds to the Nyquist frequency (half of the sampling frequency).

The figure shows that the filter 1 acts as a low pass filter, the filter 2 serves as a band-pass filter and the filter 3 can be taken as a high-pass filter. Hence, by passing through these three filters, the original signal is split into three sub-signals and each sub-signal holds a different frequency content of the original signal $f(t)$: A_2 conserves most low-frequency content of $f(t)$, that is why it is called 'approximation'; D_1 contains the high-frequency content of $f(t)$, that is why it is called 'detail'; D_2 is another detail signal including the information of $f(t)$ which is not contained in A_2 and D_1. In this case, D_2 covers most of the middle-frequency content. These details and approximations at various levels may reveal valuable information of the signal characteristics that may not be clearly seen in the original signal $f(t)$.

2.2. Two-dimensional wavelet transform (2D-WT)

The two-dimensional (2D) wavelet representation is a straightforward generalisation of the one-dimensional (1D) wavelet representation. As in 1D, a 2D signal $f(x, y)$ can also be represented in terms of wavelet families. One difference between the 2D-WT in comparison with the 1D version is that all the signals in these wavelet families are 2D signals. In 1D wavelets, the mother wavelet family is generated by a basis wavelet function, i.e. a mother wavelet $\psi(t)$, and the father wavelet
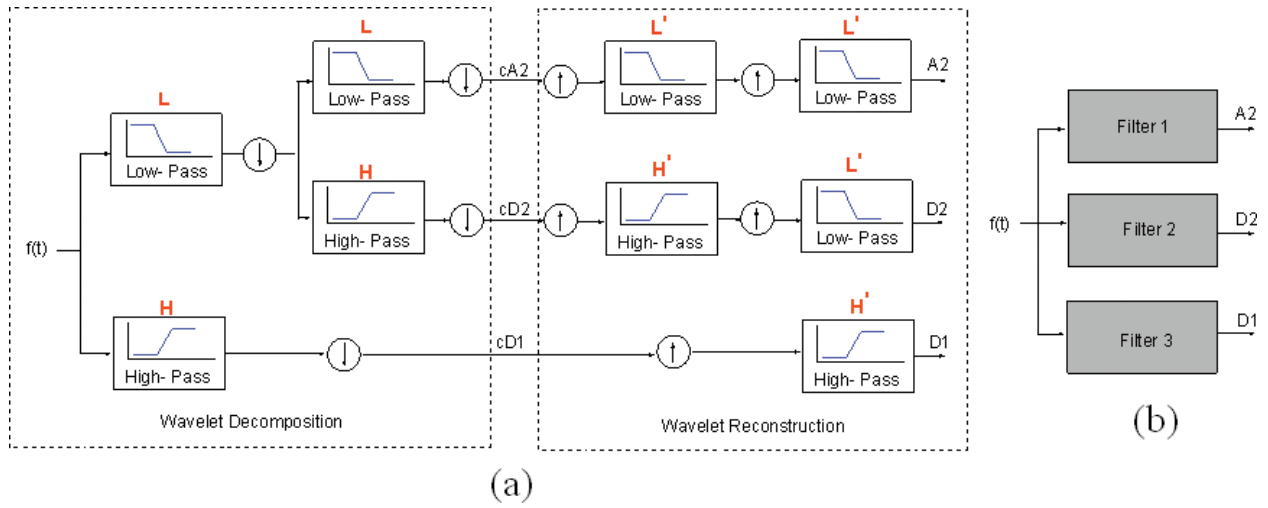
Figure 1. Filtering process of DWT and IDWT. (a) Two-level DWT decomposition and IDWT reconstruction using filter banks and (b) the three filters in (a).
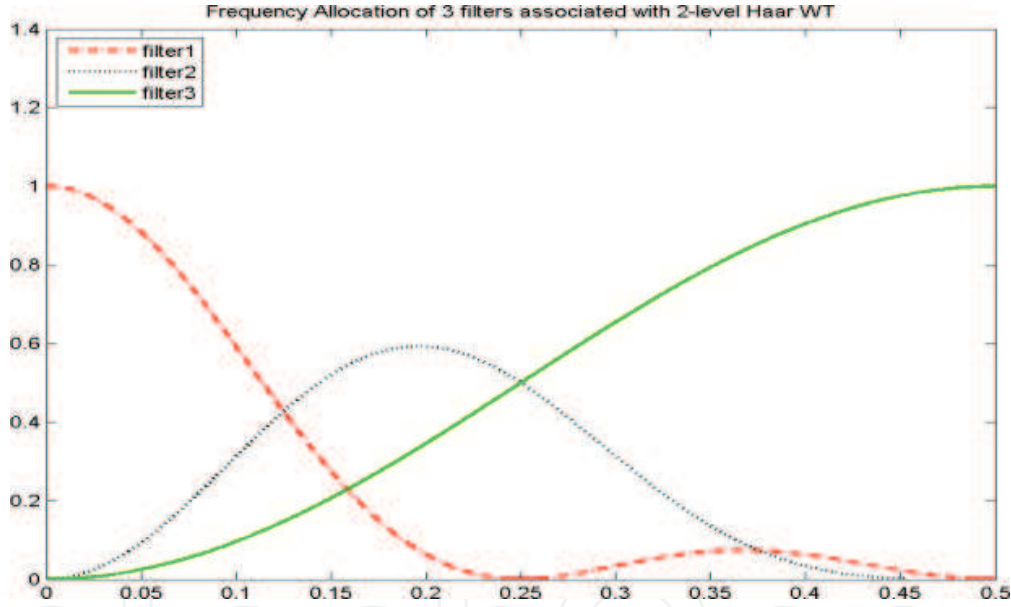
Figure 2. Frequency spectrum of the three filters associated with a two-level Haar wavelet analysis.

family is generated by another basis wavelet function, i.e. a father wavelet $\varphi(t)$. Similarly, in 2D-WT, wavelet families can also be generated from basis 2D wavelet functions [21, 22]. These basis 2D wavelet functions can be constructed by taking the tensor product (denoted as '$\otimes$' in the following equations) of a horizontal basis 1D wavelet function and a vertical basis 1D wavelet function. This leads to four different types of 2D basis wavelet functions:

$$\Phi(x, y) = \varphi_h(x) \otimes \varphi_v(y) = \text{horizontal father} \otimes \text{vertical father} \tag{2a}$$

$$\Psi^v(x, y) = \psi_h(x) \otimes \varphi_v(y) = \text{horizontal mother} \otimes \text{vertical father} \tag{2b}$$

$$\Psi^h(x, y) = \varphi_h(x) \otimes \psi_v(y) = \text{horizontal father} \otimes \text{vertical mother} \tag{2c}$$

$$\Psi^d(x, y) = \psi_h(x) \otimes \psi_v(y) = \text{horizontal mother} \otimes \text{vertical mother} \tag{2d}$$

From Eq. (2a) to (2d), the basis 2D wavelet functions include one father wavelet and three mother wavelets. The corresponding four 2D wavelet families $\{\Phi_{m,n}(x,y)\}$, $\{\Psi_{j,m,n}^{v}(x,y), j \geq 0\}$, $\{\Psi_{j,m,n}^{h}(x,y), j \geq 0\}$ and $\{\Psi_{j,m,n}^{d}(x,y), j \geq 0\}$ are generated by scaling and translating these four-basis 2D wavelet functions as follows:

$$\Phi_{m,n}(x,y) = \Phi(x-m, \ y-n) \tag{3a}$$

$$\Psi_{j,m,n}^{v}(x,y) = 2^{-j}\Psi^{v}(2^{-j}x-m, \ 2^{-j}y-n) \tag{3b}$$

$$\Psi_{j,m,n}^{h}(x,y) = 2^{-j}\Psi^{h}(2^{-j}x-m, \ 2^{-j}y-n) \tag{3c}$$

$$\Psi_{j,m,n}^{d}(x,y) = 2^{-j}\Psi^{d}(2^{-j}x-m, \ 2^{-j}y-n) \tag{3d}$$

As with 1D wavelets, the father wavelet family is good at representing the smooth part and the mother wavelets are good at representing the details of a 2D signal. Hence, in 2D wavelets, the father wavelet family $\{\Phi_{m,n}(x,y)\}$ is used to describe the smooth part of $f(x,y)$, and three mother wavelet families, $\{\Psi_{j,m,n}^{v}(x,y), \ j \geq 0\}$, $\{\Psi_{j,m,n}^{h}(x,y), \ j \geq 0\}$, and $\{\Psi_{j,m,n}^{d}(x,y), \ j \geq 0\}$, are used to capture the vertical detail, the horizontal detail, and the diagonal detail of $f(x, y)$, respectively.

2.3. Adaptive network-based fuzzy inference system (ANFIS)

The combination of artificial neural networks (ANN) and fuzzy inference systems (FIS) has attracted the interest of researchers in various scientific and engineering areas due to the growing need of adaptive intelligent systems to solve real-world problems. ANNs learn by adjusting the interconnections between layers. FIS is a popular computing framework based on the concept of fuzzy set theory, fuzzy if-then rules, and fuzzy reasoning. There are several approaches that integrate ANN and FIS, and ANFIS is one of them. ANFIS can be treated as a FIS with a network-like structure or as an ANN containing fuzzy rules. Due to that, by adopting ANFIS in the form of an ANN clearly reveals its training ability, this form of treating ANFIS is explained as follows. For the explanation of ANFIS as a FIS, the interested reader is referred to Ref. [23]. For simplicity, it is assumed that a zero-order Sugeno fuzzy model has been adopted in the ANFIS structure. Hence, the ANFIS under consideration has two inputs x and y and one output z. Each input is assumed to have two fuzzy sets defined as their possible values, from the FIS point of view. Therefore, the ANFIS structure in this case can be seen as the five-layer ANN shown in **Figure 3**. The output of the ith node in layer j is denoted as O_i^j.
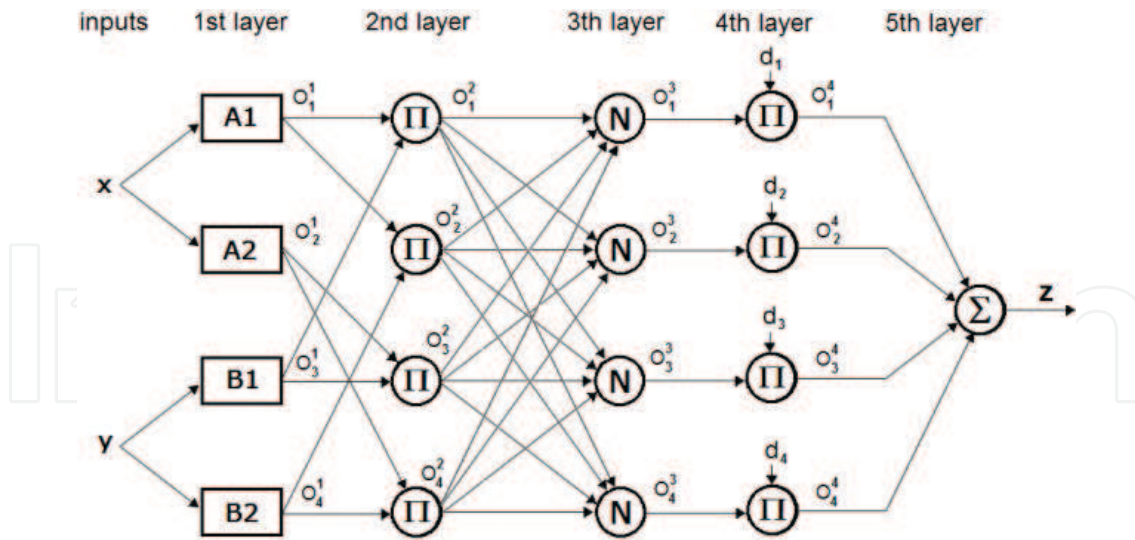
The function of each layer is as follows:

Layer 1: The function of nodes in the first layer is equivalent to the 'fuzzification' process in a fuzzy system.

$$O_i^1 = \mu_{A_i}(x), \ \text{for } i = 1, 2 \tag{4a}$$

$$O_i^1 = \mu_{B_{i-2}}(y), \text{for } i = 3, 4 \tag{4b}$$

Figure 3. ANFIS architecture for a two-input Sugeno fuzzy model with four rules (from ANN point of view).

where μ_{A_i} and $\mu_{B_{i-2}}$ are the activation functions or membership functions (MF) defining the fuzzy sets for the inputs x and y, respectively.

Layer 2: Every node in this layer generates an output which is the product of all the incoming signals to that node. This process is equivalent to applying an 'AND' operator in the counterpart fuzzy system.

$$O_i^2 = O_1^1 O_{i+2}^1, \text{ for } i = 1, 2 \tag{5a}$$

$$O_i^2 = O_2^1 O_i^1, \text{ for } i = 3, 4 \tag{5b}$$

The output of this layer O_i^2 is the w_i, i^{th} firing strength, in the fuzzy system.

Layer 3: The ith node in this layer calculates the ratio between the output of the ith node in the previous layer and the sum of the outputs of all nodes in that layer:

$$O_i^3 = \frac{O_i^2}{\sum\limits_{j=1}^{4} O_i^2} \tag{6}$$

The step in the counterpart fuzzy system is the normalisation of firing strengths.

Layer 4: Every node in this layer has a function of $O_i^4 = d_i O_i^3$, which applies the normalised firing strength (O_i^3) to the corresponding consequent parameter (d_i). The function of this layer corresponds to applying the implication method from a FIS point of view.

Layer 5: For the current ANFIS, there is only one node in this output layer. The node computes the overall ANFIS output through the summation of all incoming signals:

$$O^5 = \sum_{i=1}^{4} O_i^4 \tag{7}$$

The function of this node combines the steps of aggregation and defuzzification from the FIS point of view. Therefore, given a training set (input and output data pairs), ANFIS adjusts its parameters using well-developed learning algorithms. The parameters to be estimated in ANFIS are the premise parameters which define the membership functions in Layer 1, and the consequent parameters in Layer 4. ANFIS uses a hybrid-learning algorithm to estimate these parameters: a back-propagation learning algorithm is used to determine the premise parameters and least mean square estimation is adopted to determine the consequent parameters [23].

3. Multi-sensor data fusion and feature extraction using 2D-WT

The most common, as well as the most successful, application of 2D-WT is image compression. For instance, 2D-WT-based compression algorithms for transmitting and storing digitised fingerprints have been widely studied and used in the last decade [24, 25]. However, not much literature can be found of using the 2D-WT in structural health monitoring. In most applications, a set of many sensors are placed along different sections of a structure to measure its vibration response, accordingly the information from all the sensors needs to be integrated in some meaningful way. In this section, a novel method of using 2D-WT to carry out damage detection and localisation tasks is introduced. The 2D-WT provides an efficient and natural way to simultaneously extract features and integrate the information of many sensors, which makes the structural damage identification reliable and efficient.

The main idea of using the 2D-WT as a feature extraction and sensor data fusion mechanism is as follows: the structural response measured by one sensor i is a vector denoted as:

$$f_i(t) = [f_i(t_1) \quad f_i(t_2) \quad \dots \quad f_i(t_n)]^T \tag{8}$$

where n denotes the sampling number. Without losing any generality, it is assumed that l sensors (from sensor 1 to sensor l) are used to measure the vibration response of the structure under consideration. Thus, there are l measurement response vectors $\{f_1(t), f_2(t) \dots f_l(t)\}$. If these vectors are concatenated along rows and the result denoted as F, it gives:

$$F = [f_1(t) \quad f_2(t) \quad \dots \quad f_l(t)] \tag{9}$$

with F being an n-by-l matrix, which can be seen as an image, a 2D signal. A certain column of this image represents n vibration response samples measured by a sensor at some particular point of the structure, and a certain row of this image represents the vibration response samples measured by each sensor at l different location points of the structure at a particular sample time. The image F includes the information provided by all of the sensors throughout the measurement experiment duration and therefore gives a whole picture describing the dynamic behaviour of the structure under study. Therefore, if 2D-WT is applied to image

F, then its important features are revealed. A feature vector can be formulated in the following way: at the L-level 2D-WT, the original 2D signal (image) F is decomposed into $1 + 3L$ sub-2D signals (images): i.e. A_1, D_1^v, D_1^h, D_1^d, for a level 1 2D-WT decomposition.

The ratio of energy content of the $1 + 3L$ sub-signals in F is then defined as:

$$V = \left[\frac{\varepsilon_1}{\varepsilon_f}, \frac{\varepsilon_2}{\varepsilon_f} .... \frac{\varepsilon_{1+3L}}{\varepsilon_f} \right] \qquad (10)$$

By arranging the 2D signal as a 1D signal, the terms $\varepsilon_1, \varepsilon_2, ...\varepsilon_{1+3L}$ in Eq. (10) are calculated using:

$$\varepsilon_x \stackrel{def}{=} \sum_{n=1}^{N} |x_n|^2 \qquad (11)$$

which determines the energy of a discrete signal $x = [x_1, x_2, ..., x_N]^T$. The $\varepsilon_1, \varepsilon_2, ..., \varepsilon_{1+3L}$ terms represent the energy content in the sub-signals obtained from the 2D-WT. The term ε_f is the energy content in the original signal F. Each one of the components of V represents the energy percentage content of each of the $1 + 3L$ sub-signals in F. Therefore, a feature vector can be formed selecting some p components of V, which in turns would mean choosing some of the sub-2D signals as significant sub-signals contributing large energy percentages in F. The selection can be based on the following two criteria:

1. The sub-signals selected should be significant sub-signals contributing large energy percentages in F. The reason for this criterion lies in the fact that the insignificant sub-signals generated by WT are normally contributing to noise and should be removed. Empirically, it is assumed that a sub-signal is significant if its ratio of energy contribution to the original signal is no less than 3%.

2. The sub-signals selected should be sensitive to the damage. Damage usually has different effects on different frequency bands. For example, the effect of a crack on a beam is only noticeable within a high frequency band. Hence different sub-signals have different sensitivities to damage. By selecting the sub-signals sensitive to the damage, it is guaranteed that the damage could be effectively captured. The sensitivity analysis can be derived either by finite element modal analysis of the structure (analytical method) or by prior experiments (experimental method).

Although the two criteria above can be used, in this study, for convenience, we only choose the significant sub-signals, the ones with higher energy percentage content values, to form the feature vector.

Having chosen the energy percentage vector as the feature, the procedures for damage identification depend on the availability of the *a-priori* data. In an 'unsupervised learning mode', where data are only available from the undamaged structure, damage identification methods are based on feature comparison: two features, one extracted from the system in undamaged condition and the other from the current system, are compared in some way to obtain the

damage indicator. The damage indicator is then compared to some threshold value and the conclusion about if the structure has deviated from the reference condition is obtained. On the other hand, in a 'supervised learning mode', where data from a system in different structural conditions (including the undamaged and some damaged conditions) are known in advance, the damage identification techniques are based on pattern classification: a database including models of the structure in different conditions is established using feature vectors for the *a-priori* data sets. Given a new data set which is to be classified as one of the conditions of the system, the task is to search through the database for the model which gives the best fit to the data. The corresponding condition of this database model is then applied to the data.

4. Structural damage detection combining 2D-WT and ANFIS

In this section, a detailed description on how to use the proposed ANFIS-2D-WT feature extraction method in structural damage identification is presented. As described before, the measurements of all the sensors are processed at the same time. Firstly, the measurements from all the l sensors in each test are arranged as a matrix and seen as a 2D signal (image), as it was explained in Section 3. Therefore, let us assume that the number of all possible conditions for the system is $r + 1$ (one healthy condition denoted as D_0 and r damaged conditions $D_1 : D_r$). It is assumed also, that for each condition, and considering all the sensors, a total of N images, or 2D data measurements are available. This results altogether in $(r + 1) \times N$ image data sets that can be arranged as a data matrix:

$$Data\ Matrix\ 2D = \begin{bmatrix} \{\alpha^{D_0\_1}\}, & \{\alpha^{D_0\_2}\}, & \ldots & \{\alpha^{D_0\_N}\} \\ \{\alpha^{D_1\_1}\}, & \{\alpha^{D_1\_2}\}, & \ldots & \{\alpha^{D_1\_N}\} \\ . & . & . & . \\ . & . & . & . \\ \{\alpha^{D_r\_1}\}, & \{\alpha^{D_r\_2}\}, & \ldots & \{\alpha^{D_r\_N}\} \end{bmatrix} \qquad (12)$$

where the 2D signals $\{\alpha^{D_j\_i}\}(i = 1\ldots N, j = 0\ldots r)$ correspond to output measurement data images from the ith test at condition D_j (2D signals, considered as images) from all the sensors. Each row of the matrix contains all the available image data sets for a certain condition.

Then, select a typical measurement 2D signal (or image) $\{\alpha\}$ in the data matrix and perform 2D-WT analysis on it. The original 2D signal $\{\alpha\}$ is decomposed into a number of sub-2D signals and the energy percentage contribution of each sub-2D signal into the original 2D signal is calculated. Based on the calculated energy percentages, p sub-signals are selected and the corresponding energy percentage feature vector is formulated. The energy percentages of the selected sub-signals are the inputs to the ANFIS model. Therefore, the number of input variables to the ANFIS is p. Three linguistic values characterised using linguistic terms as 'small', 'medium' and 'large' are defined for each of the p input variables. The type of these MFs for these linguistic values is 'bell-shape' and is defined by:

$$\mu_s(x) = \frac{1}{1 + |\frac{x - c_i}{a_i}|^{2b_i}} \qquad (13)$$

Note that the linguistic values such as 'small', 'medium' or 'large' have different meanings for different input variables. There is only one output variable defined in the ANFIS: the structural health condition. For convenience, it is normally represented by a condition index. A zero-order Sugeno fuzzy model has been adopted in the ANFIS structure, which means that singleton values are defined for the output variable and the type of the corresponding MF is a distinct constant. So far, only the architecture of the ANFIS model has been determined: it contains p inputs (corresponding to p energy percentages) and one output (condition index). Each input variable has 'small', 'medium' and 'large' linguistic values characterized by three bell-shape MFs. The number of ANFIS rules is determined by the combination of linguistic values for the input variables. For p input variables, each with three linguistic values, the number of resultant combinations is 3^p. Correspondingly, the number of rules is 3^p. For example, assume that only two sub-signals are selected ($p = 2$). The two input variables and one output variable are denoted respectively as x_1, x_2 and z. For each input variable, three linguistic values denoted as $\{M_1^{x_1}, M_2^{x_1}, M_3^{x_1}\}$ (for x_1) and $\{M_1^{x_2}, M_2^{x_2}, M_3^{x_2}\}$ (for x_2) are defined. Therefore, a total of nine rules are contained in the ANFIS model:

Rule 1: If x_1 is $M_1^{x_1}$ *and* x_2 is $M_1^{x_2}$, then z is d_1

Rule 2: If x_1 is $M_1^{x_1}$ *and* x_2 is $M_2^{x_2}$, then z is d_2

Rule 3: If x_1 is $M_1^{x_1}$ *and* x_2 is $M_3^{x_2}$, then z is d_3

Rule 4: If x_1 is $M_2^{x_1}$ *and* x_2 is $M_1^{x_2}$, then z is d_4

....

Rule 9: If x_1 is $M_3^{x_1}$ and x_2 is $M_3^{x_2}$, then z is d_9

Once the ANFIS architecture and rules are determined, it is necessary to prepare data sets for training use. For each available output data $\{y^{D_j\_i}\}$ ($i = 1\ldots N, j = 0\ldots r$) in the data matrix, perform the same 2D-WT analysis and the same p sub-signals are selected to form the feature vector. Their energy percentages are arranged as a vector denoted as $Per^{D_j\_i}$. This procedure is applied to all the data set in Eq. (12), and a matrix referred to as energy percentage matrix (EPM) is obtained:

$$EPM(WPT) = \begin{bmatrix} \{Per^{D_0\_1}\}, & \{Per^{D_0\_2}\}, & \ldots & \{Per^{D_0\_N}\} \\ \{Per^{D_1\_1}\}, & \{Per^{D_1\_2}\}, & \ldots & \{Per^{D_1\_N}\} \\ . & . & . & . \\ . & . & . & . \\ \{Per^{D_r\_1}\}, & \{Per^{D_r\_2}\}, & \ldots & \{Per^{D_r\_N}\} \end{bmatrix} \quad (14)$$

The vector $\{Per^{D_j\_i}\}$, containing p elements, is taken as an input vector for the ANFIS. EPM Matrix contains a total of $(r + 1) \times N$ such input vectors for ANFIS. They are used as training data for ANFIS. The current ANFIS use a supervised learning algorithm, which means that the target output for each input vector is needed. It has been mentioned earlier that the ANFIS output is the structural condition represented by a condition index. Depending on the level of damage assessment conducted, different output index patterns are adopted. If the ANFIS is used only to identify damage occurrence (level 1 damage assessment), the output indices are Boolean values (0 for healthy condition D_0, 1 to r for damaged cases $D_1{\sim}D_r$). In this situation, the EPM data matrix can be appended to contain a total of $(r + 1) \times N$ input and desired output data pairs:

$$Data\ Matrix(Level\ 1) = \begin{bmatrix} \{Per^{D_0\_1}, 0\}, & \{Per^{D_0\_2}, 0\}, & \dots & \{Per^{D_0\_N}, 0\} \\ \{Per^{D_1\_1}, 1\}, & \{Per^{D_1\_2}, 1\}, & \dots & \{Per^{D_1\_N}, 1\} \\ . & . & . & . \\ . & . & . & . \\ \{Per^{D_r\_1}, 1\}, & \{Per^{D_r\_2}, 1\}, & \dots & \{Per^{D_r\_N}, 1\} \end{bmatrix} \quad (15)$$

If the ANFIS is used for the damage localisation (level 2 damage assessment), a total of $r + 1$ condition indices each corresponding to a structural condition need to be defined. Defining j as the index for condition D_j, the data matrix containing the input and desired output data pairs is:

$$Data\ Matrix(Level\ 2) = \begin{bmatrix} \{Per^{D_0\_1}, 0\}, & \{Per^{D_0\_2}, 0\}, & \dots & \{Per^{D_0\_N}, 0\} \\ \{Per^{D_1\_1}, 1\}, & \{Per^{D_1\_2}, 1\}, & \dots & \{Per^{D_1\_N}, 1\} \\ . & . & . & . \\ . & . & . & . \\ \{Per^{D_r\_1}, r\}, & \{Per^{D_r\_2}, r\}, & \dots & \{Per^{D_r\_N}, r\} \end{bmatrix} \quad (16)$$

Data matrices Level 1 and Level 2 (Eqs. (15) and (16)) are used, respectively, for training ANFIS with two different levels of damage assessment.

The next step is ANFIS training. The number of the premise parameters to be determined is $3 \times 3 \times p$. This comes from the fact that for each of the p input variables, three MFs, each defined by three premise parameters, were established. The number of the consequent parameters to be determined is 3^p. The ANFIS architecture uses a hybrid learning algorithm [23] to estimate these $9p + 3^p$ premise parameters all together with the consequent parameters.

Usually, in the implementation of a structural health monitoring system, a large number of sensors on the structure under analysis are strategically placed to provide an early indication of damage. The problem then is the processing of the signals collected from all the sensors. This problem is approached in this work by using the 2D-WT to process all the information provided by the sensors at once. This is possible by integrating all the signals into a matrix that can be considered as a 2D image. In this way the information provided by each sensor individually is taken into account, preserved and fused with the information from the other sensors.

ANFIS is used for the purpose of structural damage identification. However, there are various levels of damage assessments. Two ANFIS models, ANFIS1 and ANFIS2 are established accordingly. ANFIS1 is used to identify damage occurrence (level 1 damage assessment) while ANFIS2 is used for damage localisation (level 2 damage assessment). The architecture of these two ANFIS models is the same, but they produce different output values. ANFIS1 is only used to distinguish healthy and damaged conditions; therefore the output is a Boolean value (0 for healthy, 1 for damaged). The output of ANFIS2 is designed to differentiate all the possible conditions, which is performed by defining a numerical value j ($j = 0$ to 5), where j corresponds to damage condition D_j.

5. Experimental setup with a cantilever beam

For the sake of repeatability and insight, cantilevered beam experiment settings have been used by several researchers to demonstrate the feasibility of their proposed approaches to

damage detection and localisation using a plethora of techniques, examples include Refs. [26–28]. Furthermore, several aerospace and civil structures such as rotor blades and bridges could be modelled as cantilever beams. Therefore, in this section the results of an experimental study involving shaker-excited vibration tests of an aluminium cantilever beam carried out in the laboratory are presented. The beam is 90 cm length and cross-section 2.545×0.647 cm. Zero-mean band-limited (0–500 Hz) Gaussian white noise was used as the input signal to the amplifier. The amplifier gain was controlled manually and the shaker provided an approximately 10 N peak, via a random force input to the beam. A force gauge screwed on the bottom surface of the beam was used to directly measure the input. The shaker was attached with this force transducer through a stinger. **Figure 4** shows the experimental setup.

Six accelerometers (7 g each) were screwed to the top surface along the centreline at selected positions (15, 30, 45, 60, 75, and 90 cm from the left fixed point, respectively). The data from each test came from these six accelerometers and one force transducer. The data were collected at a sampling rate of 10 kHz for a duration of 4 seconds. Five damage scenarios ($D1$ to $D5$) were simulated by adding a lumped mass (22 g) at 30, 45, 60, 75, and 90 cm, respectively (see **Figure 4**). A summary of the experimental damage conditions is provided in **Table 1**.
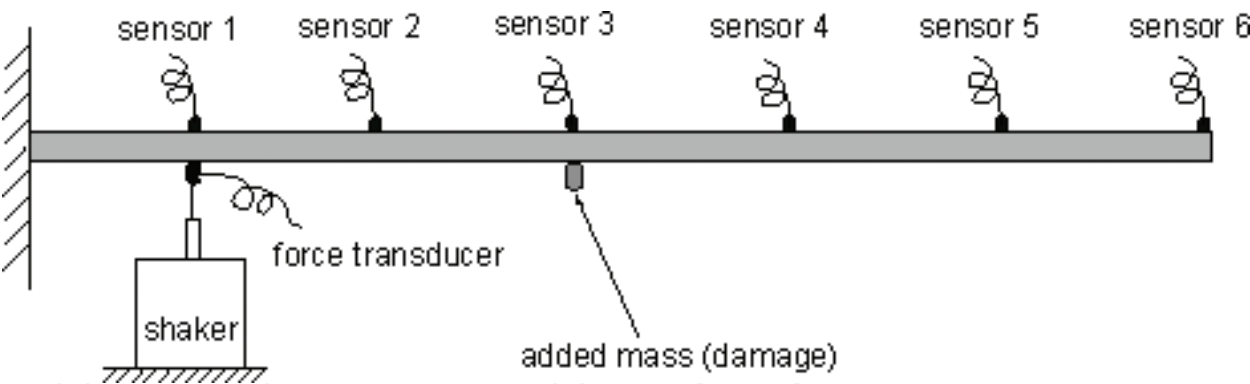
Figure 4. Cantilever beam experiment; setup schematic representation.

Damage case	Location of damage	Damage description
D1	0.30 m	Adding a lumped mass of 0.022 kg
D2	0.45 m	Adding a lumped mass of 0.022 kg
D3	0.60 m	Adding a lumped mass of 0.022 kg
D4	0.75 m	Adding a lumped mass of 0.022 kg
D5	0.90 m	Adding a lumped mass of 0.022 kg

Table 1. Summary of damage case D1–D5: adding a lumped mass at different locations.

6. Results

The experiment was repeatedly carried out under each of the six possible conditions of the system. The system response data and the corresponding condition were recorded during the test. From each condition, 20 test data are used, within which the first 10 are for the training use and the remaining 10 are for the testing use. Therefore, altogether there are 60 training data sets and 60 test data sets available. Thus, ANFIS is used for the purpose of structural damage identification. However, there are various levels of damage assessments. Two ANFIS models, ANFIS1 and ANFIS2 are established accordingly. ANFIS1 is used to identify damage occurrence (level 1 damage assessment) while ANFIS2 is used for damage localisation (level 2 damage assessment). The architecture of these two ANFIS models is the same, but they produce different output values. ANFIS1 is only used to distinguish healthy and damaged conditions; therefore the output is a Boolean value (0 for healthy, 1 for damaged). The output of ANFIS2 is designed to differentiate all the possible conditions, which is performed by defining a numerical value j (j = 0–5), where j corresponds to damage condition D_j.

As previously described, in the proposed ANFIS-2D-WT method the measurements from all six sensors in each test are arranged as a matrix. The two-level db3 2D-WT is performed on this matrix. From the obtained seven sub-signals, three are selected and their energy percentages are taken as inputs for ANFIS. Note that only one ANFIS1 model is needed for level 1 damage assessment and one ANFIS2 model is required for level 2 damage assessment. Each of these two ANFIS models includes the information of all six sensors. The mapping between the three inputs and one output of the trained ANFIS1 using ANFIS-2DWT method is shown in **Figure 5**. While **Figure 6** shows the results when applying the trained ANFIS1 to the testing data. In this figure, Exp means expected values, and Act means actual values. The testing error of ANFIS1 is 2.7567e-5. For the level 2 damage assessment, ANFIS-2D-WT also performs well. **Figure 7** shows the mapping relationship of the ANFIS2 model. The testing result of the trained ANFIS2 model is shown in **Figure 8**. We can see that the testing error of the ANFIS2 model is 0.0021.

The effect of noise is an influencing factor always present in the vibration response signals of structures. Therefore, to study the effect of noise on the proposed ANFIS-2D-WT method, random Gaussian white noise is added to the response of these 120 test cases. The noise intensity is defined by the signal-to-noise ratio (SNR):

$$SNR(dB) = 20\log_{10}\frac{A_{\text{signal}}}{A_{\text{noise}}} \tag{17}$$

where A_{signal} and A_{noise} refer to the root mean square (rms) amplitude of signal and noise, respectively. **Figures 9–11** show the testing results of ANFIS1 (level 1 damage assessment) with SNR = 20, 10, 5, respectively. The ratios of the RMS values between the noise and the signal for these three cases are 10, 31.6 and 56.2%, respectively. As can be seen in the figures, by using the ANFIS-2D-WT method, the damage can be correctly detected when SNR is no smaller than 10 dB.

Figures 12–14 show the testing results of ANFIS2 (level 2 damage assessment) at these noise levels. It can be seen that ANFIS2 can locate damage even when SNR = 10 dB. These
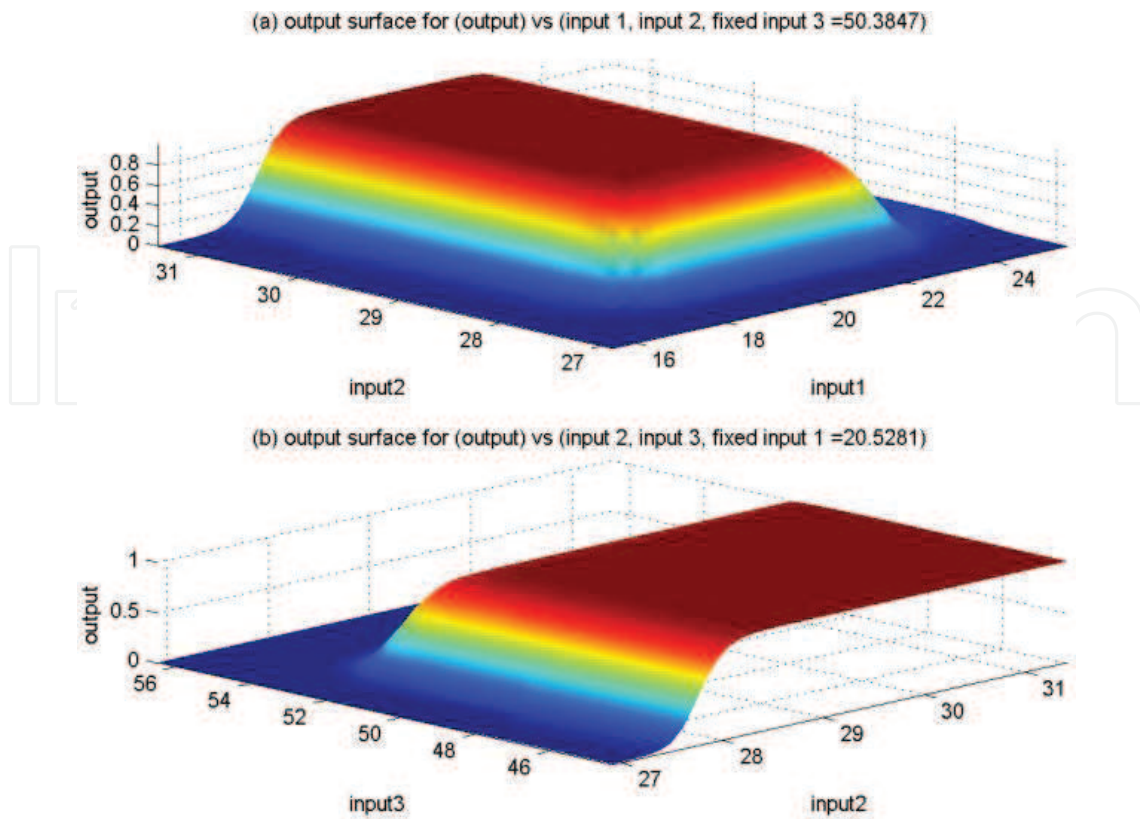
Figure 5. Output surface between ANFIS output and inputs: (a) input 3 is fixed to be 50.387 and (b) input 1 is fixed to be 20.5281 (ANFIS1, ANFIS-2D-WT method, using ALL six sensors).
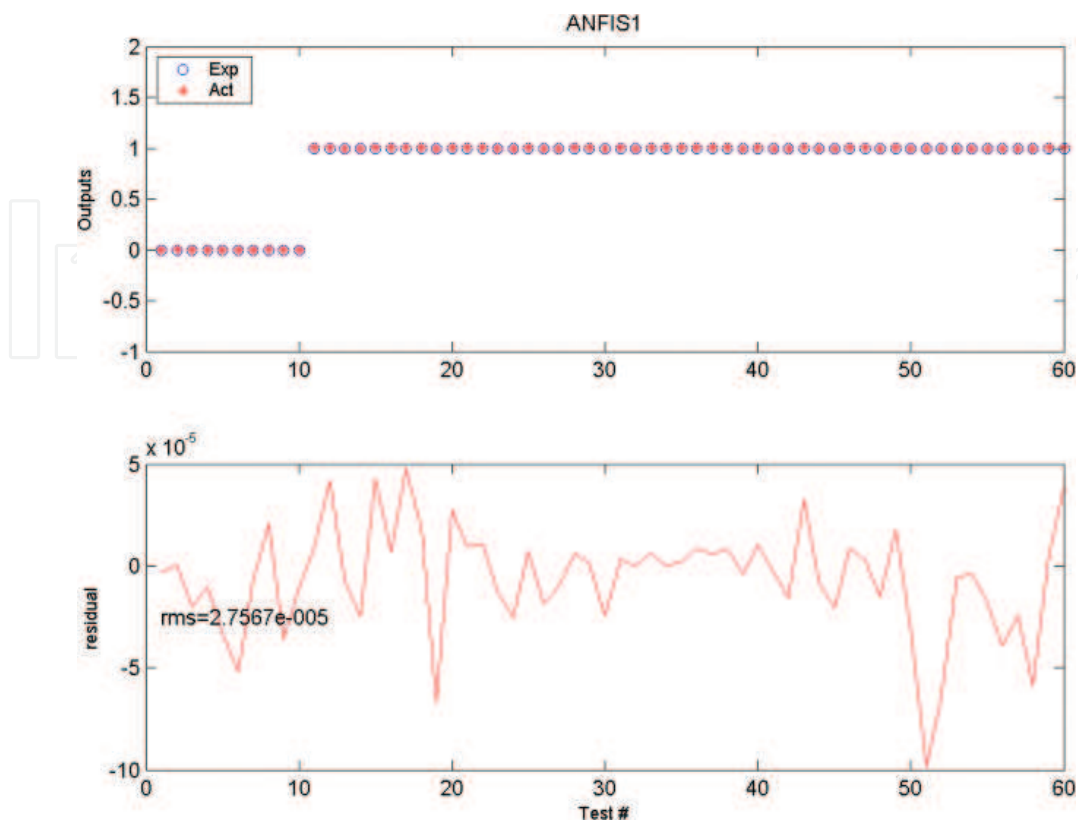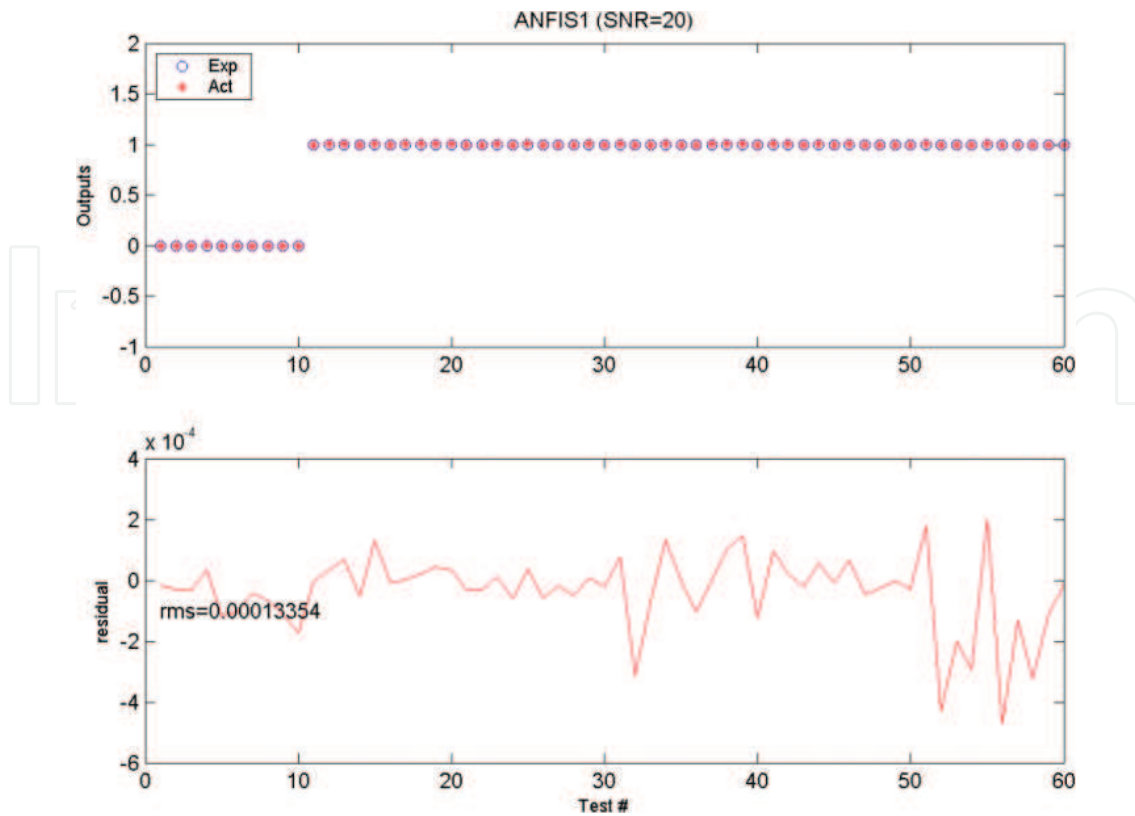

Figure 6. Testing results and the corresponding error curves (ANFIS1, ANFIS-2D-WT method, using all six sensors).
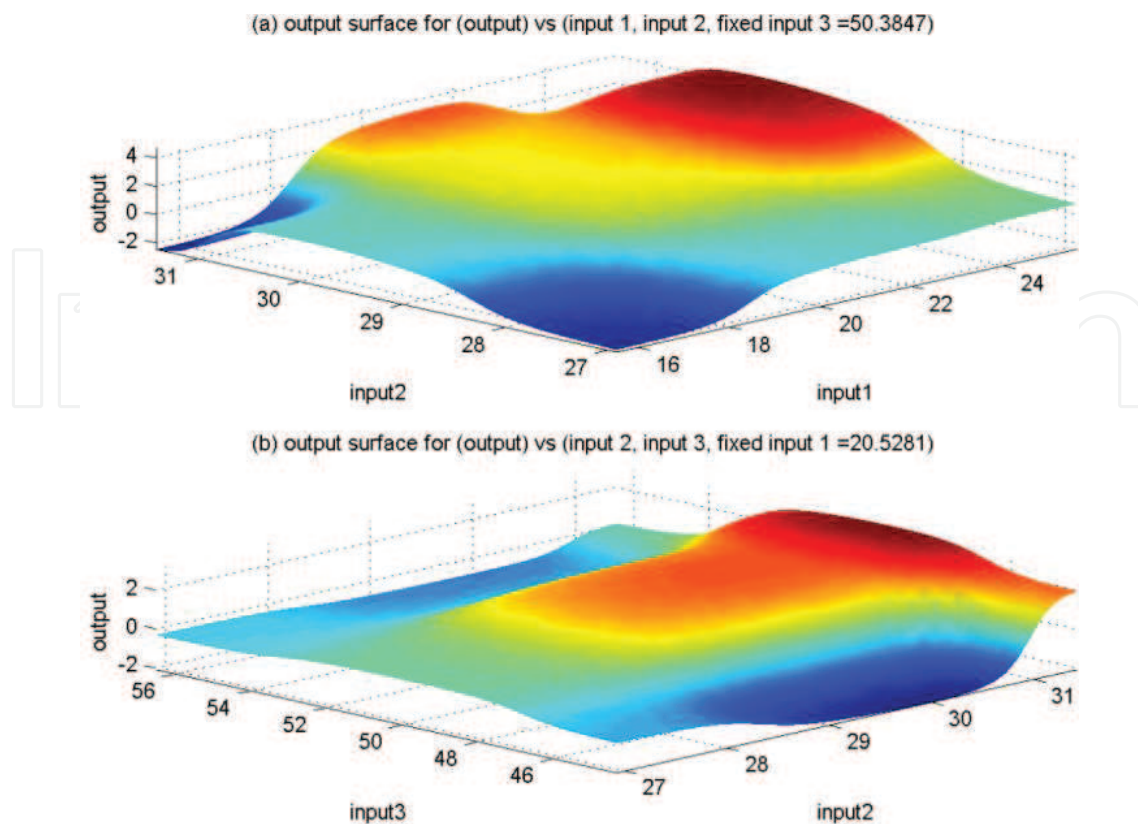
Figure 7. Output surface between ANFIS output and inputs: (a) input 3 is fixed to be 50.387 and (b) input 1 is fixed to be 20.5281 (ANFIS2, ANFIS-2D-WT method, using all six sensors).
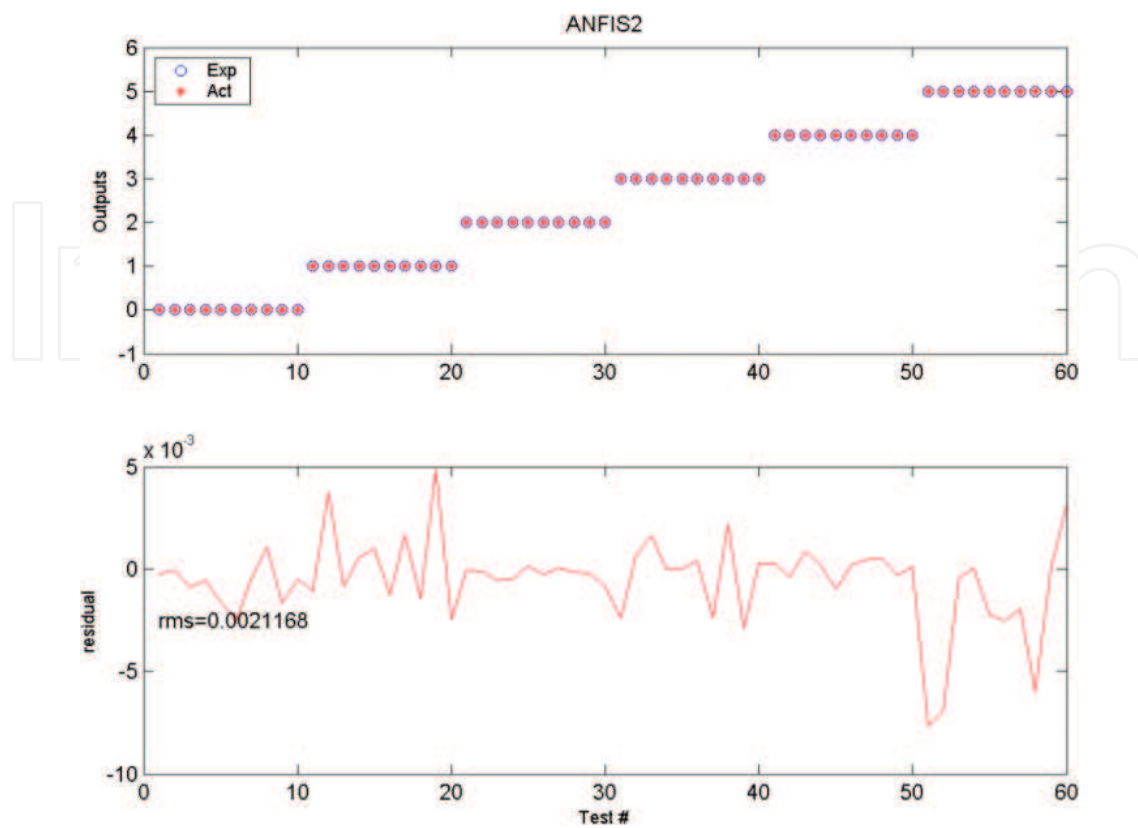
Figure 8. Testing results and the corresponding error curves (ANFIS2, ANFIS-2D-WT method, using all six sensors).

Figure 9. Testing results and the corresponding error curves (ANFIS1, ANFIS-2D-WT method, SNR = 20).
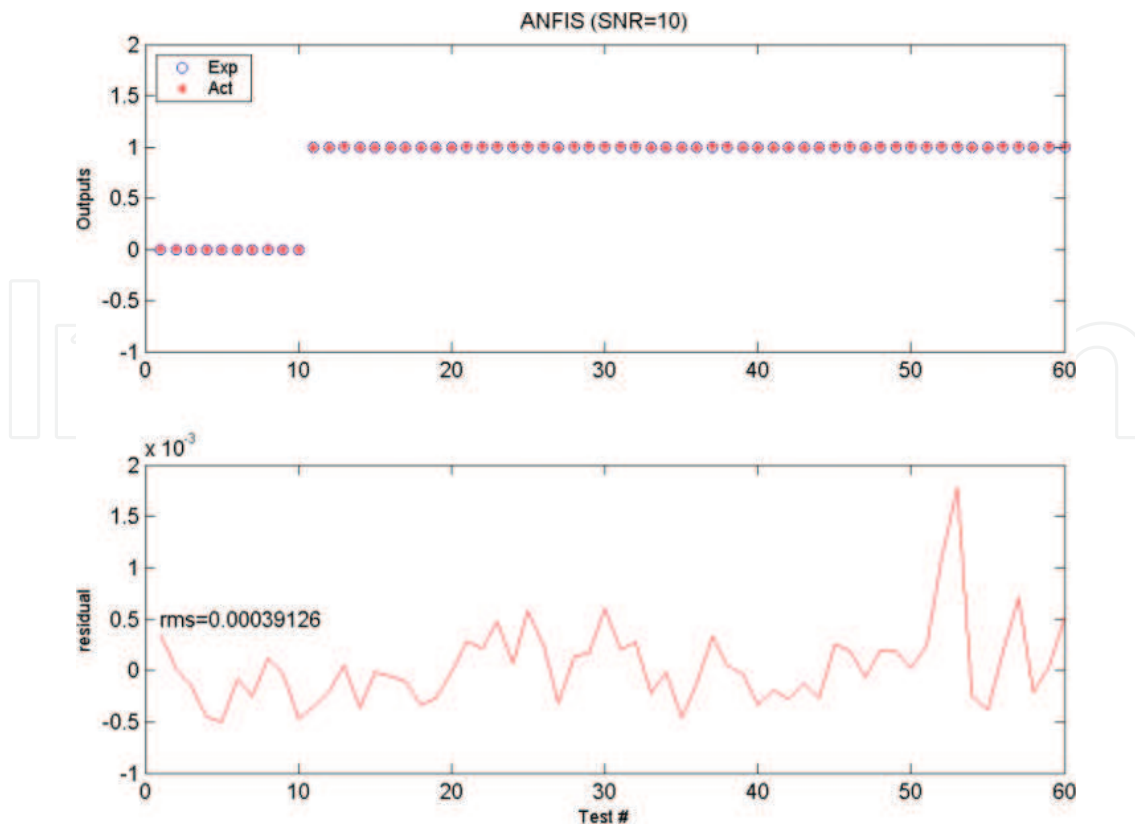
Figure 10. Testing results and the corresponding error curves (ANFIS1, ANFIS-2D-WT method, SNR = 10).
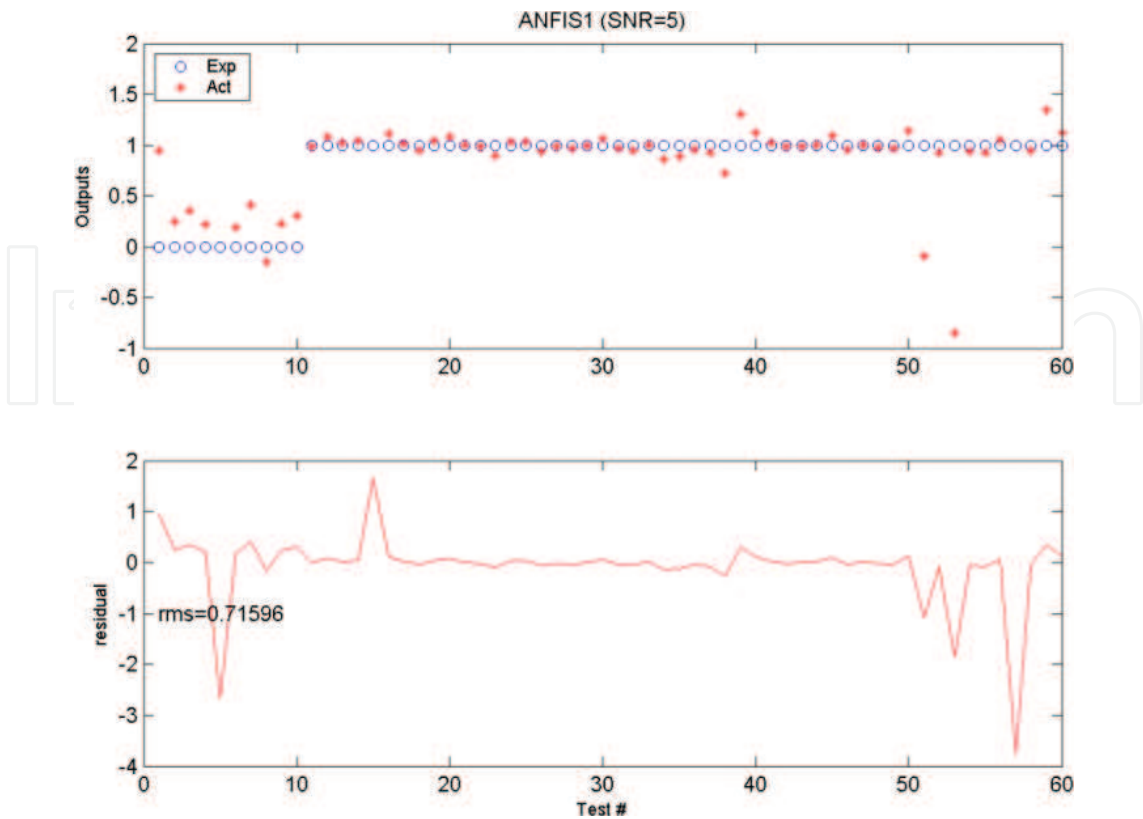
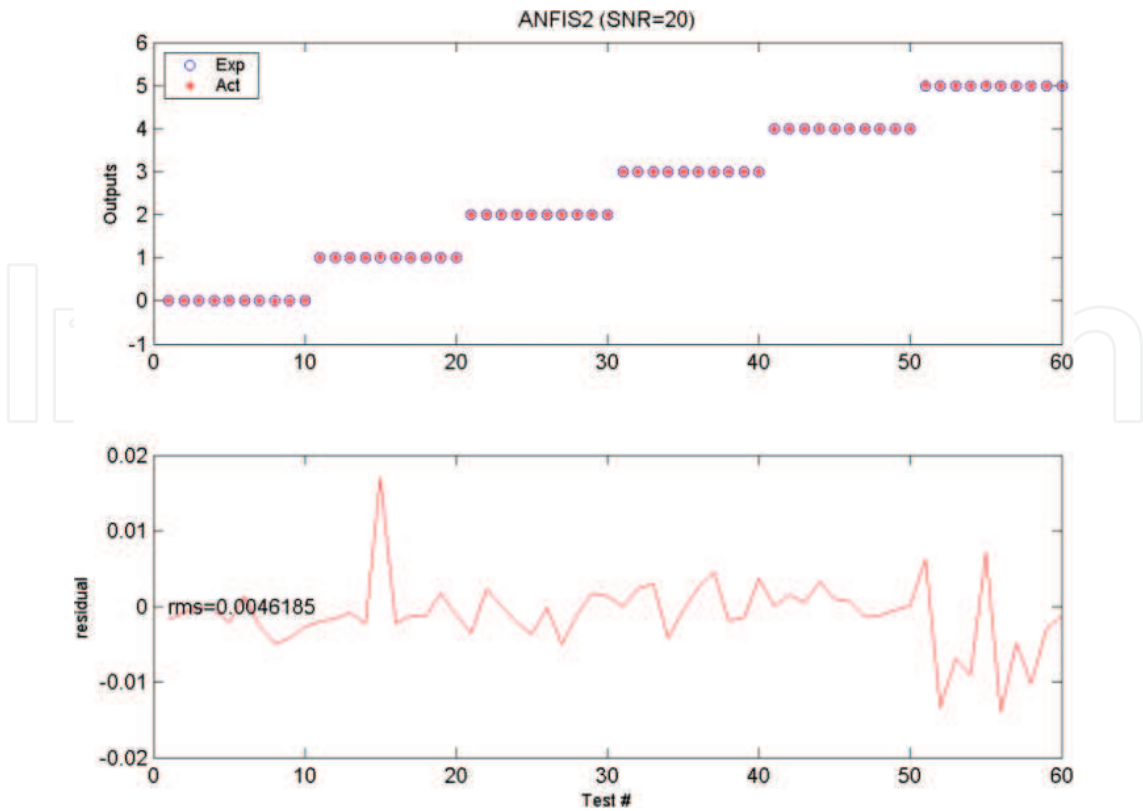**Figure 11.** Testing results and the corresponding error curves (ANFIS1, ANFIS-2D-WT method, SNR = 5).

Figure 12. Testing results and the corresponding error curves (ANFIS2, ANFIS-2D-WT method, SNR = 20).
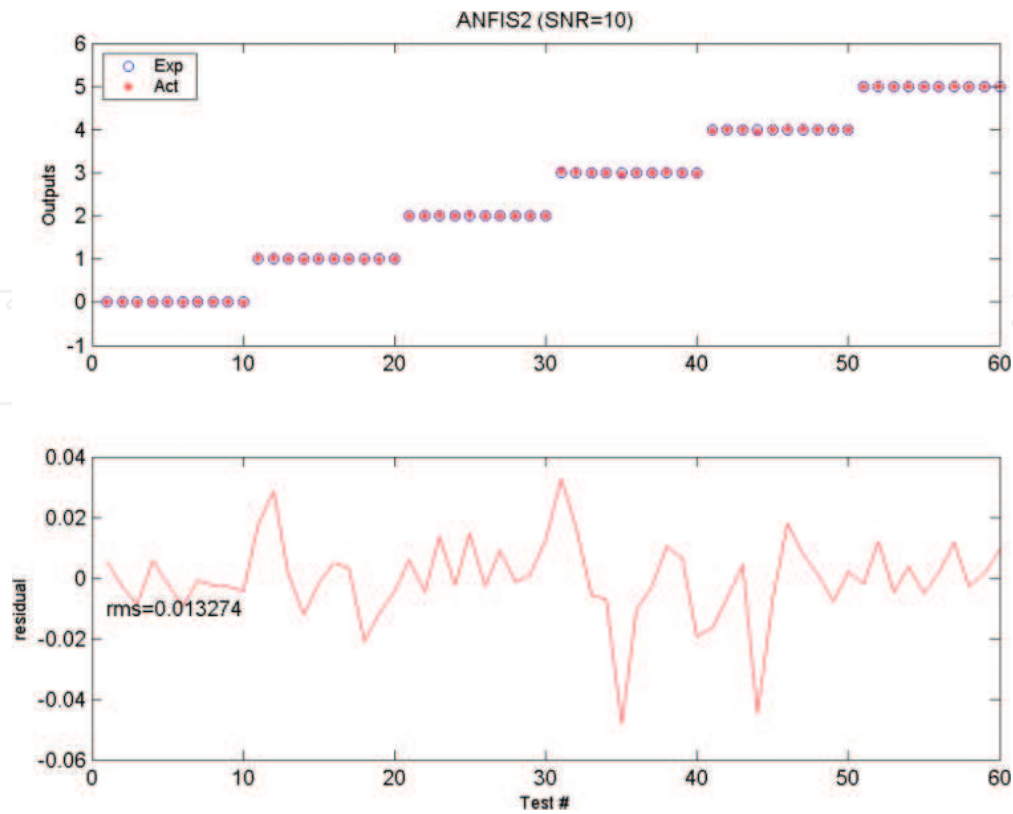
Figure 13. Testing results and the corresponding error curves (ANFIS2, ANFIS-2D-WT method, SNR = 10).
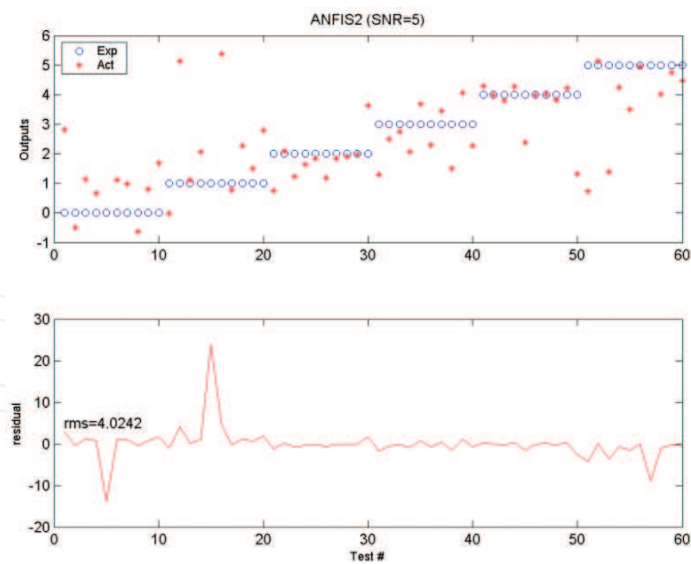

Figure 14. Testing results and the corresponding error curves (ANFIS2, ANFIS-2D-WT method, SNR = 5).

results suggest that measurement of noise does not seem to affect much of the proposed method for these two levels of damage assessment. This property can be attributed to the

wavelet transform: the effect of noise can be alleviated by choosing sub-signals less affected by noise.

7. Conclusions

In this chapter, the ANFIS and 2D-WT technologies were combined to perform structural damage identification. The structure vibration response is decomposed by 2D-WT into a number of sub-signals, from which some are selected based on their energy percentages. The energy percentages of the selected signals are taken as inputs to the ANFIS model. The output of the ANFIS is a condition index, which can be a Boolean value (0 or 1) for level 1 damage assessment use, or a number of values for level 2 damage assessment use. Provided an ANFIS model is well-trained by the available data, it can be used for health monitoring and damage localisation. The proposed feature extraction method was applied to the data from a cantilever beam for damage detection and localisation. The testing results showed that the proposed method is successful in performing the two described levels of damage assessment. In addition, the ANFIS-2D-WT can process efficiently information from many sensors at the same time, performing simultaneously multi-sensor feature extraction and data fusion. The proposed damage assessment methodology of combining ANFIS with wavelet transform has great potential to implement systems which are able to interrogate sensor measurements autonomously for indications of structural damage.

Author details

Ponciano Jorge Escamilla-Ambrosio[1]*, Xuefeng Liu[2], Juan Manuel Ramírez-Cortés[3], Abraham Rodríguez-Mota[4] and María del Pilar Gómez-Gil[5]

*Address all correspondence to: pjorgeea@gmail.com

1 Instituto Politécnico Nacional, Centro de Investigación en Computación, México, Ciudad de México, Mexico

2 Department of Computing, The Hong Kong Polytechnic University, Hung Hom, Kowloon, Hong Kong

3 Department of Electronics, National Institute for Astrophysics Optics and Electronics, Tonantzintla, Puebla, Mexico

4 Instituto Politécnico Nacional, Escuela Superior de Ingeniería Mecánica y Eléctrica Unidad Zacatenco, Ciudad de México, Mexico

5 Department of Computer Science, National Institute for Astrophysics Optics and Electronics, Tonantzintla, Puebla, Mexico

References

[1] Farrar CR, Worden K. Structural Health Monitoring: A Machine Learning Perspective, West Sussex, UK: John Wiley and Sons; 2013.

[2] Balageas D, Fritzen CP, Güemes A. Structural Health Monitoring. London: ISTE Ltd; 2006.

[3] Srinivasan G, Massimo R, Sathyanaraya H. Computational Techniques for Structural Health Monitoring. London: Springer-Verlag; 2011.

[4] Sohn H, Farrar CR, Hemez FM, Shunk DD, Stinemates DW, Nadler BR. A review of structural health monitoring literature: 1996–2001, Los Alamos National Laboratory, Report LA-13976-MS, 2003.

[5] Santos JP, Cremona C, Orcesi AD, Silveira P. Multivariate statistical analysis for early damage detection. Engineering Structures. 2013;**56**:273–285

[6] Goyal D, Pabla BS. The vibration monitoring methods and signal processing techniques for structural health monitoring: A review. Archives of Computational Methods in Engineering. 2016;23(4):585–594.

[7] Amezquita-Sanchez JP, Adeli H. Signal processing techniques for vibration-based health monitoring of smart structures. Archives of Computational Methods in Engineering. 2016;23(1):1–15.

[8] Aminpour H, Foad N, Baghalian S. Applying artificial neural network and wavelet analysis for multiple cracks identification in beams. International Journal of Vehicle Noise and Vibration. 2012;**8**(1):51-59

[9] Wei F, Qiao P. Vibration-based damage identification methods: A review and comparative study. Structural Health Monitoring. 2011;**10**(1):83-111

[10] Ganguli R. Fuzzy cognitive maps for structural damage detection. Fuzzy Cognitive Maps for Applied Sciences and Engineering, Berlin, Heidelberg: Springer; 2014. pp. 267-290

[11] Arangio S, Bontempi F. Structural health monitoring of a cable-stayed bridge with Bayesian neural networks. Structure and Infrastructure Engineering, 2015;**11**(4):575-587

[12] Katunin A. Modal-based non-destructive damage assessment in composite structures using wavelet analysis: A review. International Journal of Composite Materials. 2013;**3**(6):1-9

[13] He WY, Songye Z. Progressive damage detection based on multi-scale wavelet finite element model: Numerical study. Computers & Structures. 2013;**125**:177-186

[14] Vafaei M, Alih SC, Baharuddin A, Rahman A, Adnan AB. A wavelet-based technique for damage quantification via mode shape decomposition. Structure and Infrastructure Engineering. 2014;**11**(7):869-883

[15] Kim H, Melhem H. Damage detection of structures by wavelet analysis. Engineering Structures. 2004;**26**:347-362

[16] Facchini G, Bernardini L, Atek S, Gaudenzi P. Use of the wavelet packet transform for pattern recognition in a structural health monitoring application. Journal of Intelligent Material Systems and Structures. 2015;**26**(12):1513-1529

[17] Kim Y, Chong JW, Chon KH, Kim J. Wavelet-based AR–SVM for health monitoring of smart structures. Smart Materials and Structures. 2013; **22**(1):015003

[18] Winkelmann C, Lestari W, La Saponara V. Composite structural health monitoring through use of embedded PZT sensors. Journal of Intelligent Material Systems and Structures. 2011;**22**(8):739-755

[19] Yang Y, Nagarajaiah S. Blind identification of damage in time-varying systems using independent component analysis with wavelet transform. Mechanical Systems and Signal Processing. 2014;**47**(1):3-20

[20] Mallat S. A Wavelet Tour of Signal Processing, The Sparse Way. 3rd ed. Burlington, MA: Academic Press; 2009.

[21] Antoine JP, Murenzi R, Vandergheynst P, Ali ST. Two-dimensional wavelets and their relatives. Cambridge: Cambridge University Press; 2004.

[22] Woods JW. Multidimensional Signal, Image, and Video Processing and Coding, Second Edition. Burlington, MA: Academic Press; 2011.

[23] Jang JSR, Sun CT, Mizutani E. Neuro-Fuzzy and Soft Computing: A Computational Approach to Learning and Machine Intelligence. New Jersey: Prentice-Hall; 1997.

[24] Shanavaz KT, Mythili P. Faster techniques to evolve wavelet coefficients for better fingerprint image compression. International Journal of Electronics, 2013;**100**(5):655-668

[25] Zhao S, Song, Wang XF. Fingerprint Image Compression Based on Directional Filter Banks and TCQ. In proceedings of Second International Workshop on Knowledge Discovery and Data Mining, Moscow, Russia; 2009. pp. 660-663

[26] Nataraju M, Adams DE, Rigas EJ. Nonlinear dynamical effect and observations in modeling and simulating damage evolution in a cantilevered beam. Structural Health Monitoring, 2005; **4**(5):259-282

[27] Kim DG, Lee SB. Structural damage identification of a cantilever beam using excitation force level control. Mechanical Systems and Signal Processing, 2010;**24**:1814-1830

[28] Chen H, Kurt M, Lee YS, McFarland DM, Bergman LA, Vakakis AF. Experimental system identification of the dynamics of a vibro-impact beam with a view towards structural health monitoring and damage detection. Mechanical Systems and Signal Processing. 2014;**46**(1):91-113